Optimized Adversarial Network with Faster Residual Deep Learning for Osteoarthritis Classification in Panoramic Radiography

Vijaya Kumar Krishnamoorthy[1]*   **Santhi Baskaran[2]**

[1]*Department of Computer Engineering, Women's Polytechnic College, Puducherry, India.*
[2]*Department of Information Technology, Puducherry Technological University, Puducherry, India*
* Corresponding author's Email: mkvijayakumaramphd@gmail.com

Abstract: Temporomandibular joint osteoarthritis (TMJ-OA) is a degenerative disorder affecting the TMJ and is distinguished by the gradual deterioration of the joint's interior surfaces. To identify and classify the TMJ-OA from panoramic dental X-ray images, many deep learning models were developed. Amongst, a faster region-based convolutional neural network (FRCNN) can find the condylar area and recognize its abnormalities by learning adequate features with a limited number of images. Nonetheless, the accuracy was not effective for larger databases. Hence in this article, an optimized generative adversarial network (OGAN) model is proposed to create larger panoramic dental X-ray images for TMJ-OA recognition. This GAN model utilizes the generator to produce synthetic panoramic dental images and trains the discriminator to decide whether the created images are real or counterfeit. Besides, an Elephant Herding Optimization (EHO) algorithm is adopted to select the most optimal hyperparameters of the GAN according to the clan and separating factors. Then, the created synthetic panoramic images are added to the actual database and partitioned into 2 distinct collections: training and test collections. The training collection is utilized to train the FRCNN, which extracts the condylar area from every image and identifies the abnormalities. Further, the trained model is tested using the test set to analyze the efficiency of TMJ-OA recognition. Finally, the experimental results exhibit that the OGAN-FRCNN model achieves an accuracy of 94.59% on the panoramic dental X-ray database, whereas the classical models such as VGG16, VGG19, ResNet50, InceptionV3, DenseNet121, YOLOv3 and FRCNN achieve 83.06%, 83.81%, 85.11%, 86.92%, 89.17%, 90.85% and 92.21% accuracy, respectively.

Keywords: Temporomandibular joint, Osteoarthritis, Panoramic dental X-ray image, Deep learning, FRCNN, GAN, Hyperparameter, Elephant herding optimization.

1. Introduction

Osteoarthritis (OA) is the most common kind of arthritis that affects the TMJ. The osteoarticular region of the mandibular condyle and fossa is distorted as a result of OA. The most common cause of OA is excessive mechanical stress on joint tissue. When a continuous force is applied to the articular surface, subarticular bone resorption occurs (chondromalacia). The progressive bone change that occurs in the loss of the subchondral cortical layer and bone deterioration causes radiological osteoarthritis [1-3].

Health records, clinical diagnostics and radiographic assessment are used to examine TMJ-OA. Practically, TMJ-OA presents as restricted lower jaw movement due to pain, crepitus, and local paraspinal tenderness in the joint promotion. OA is diagnosed when a radiographic scan indicates structural bone change [4-6]. OA may also be utilized to measure the condylar and Ramal asymmetry of the mandible in those with Juvenile Idiopathic Arthritis using orthopantomography (JIA). There are several general TMJ diseases and diagnoses, which are classified as painful or non-painful [7, 8].

Panoramic radiographs are typically used in the early stages of diagnosis when bone abnormalities in the TMJ are found. However, because the TMJ has microscopic bone structures at the joint site and the joint is covered by the big skull, basic imaging is difficult to identify bone changes [9-11]. Furthermore, structural changes or lesions in the TMJ are

commonly overlooked in basic radiographs due to insufficiently dematerialized bone tissue in the early stages of OA. As a result, evaluating panoramic radiographs necessitates the use of skilled specialists with extensive clinical experience, and further radiography must be ordered as needed. Unfortunately, when medical specialists who can effectively diagnose OA based on panoramic radiographs are unavailable on-site, transferring panoramic radiographs to a professional reading expert and waiting for the findings is cumbersome.

Additionally, because a doctor cannot quickly determine the treatment state of osteoarthritis, the procedure of sending panoramic radiographs and waiting for diagnostic findings must be repeated. To combat such issues, the artificial intelligence (AI)-based model has emerged to automatically treat OA of the TMJ [12-14]. Many innovations in the AI paradigm have presented different algorithms for examining X-ray scans [15]. Convolutional neural network (CNN) technology was proven for many purposes like extracting particular sections of X-ray scans and detecting abnormalities [16-20]. Various researches on dental X-ray image analysis have been undertaken, including tooth discovery by panoramic image analysis, osteoporosis analysis, and sinusitis analysis. However, investigations relying solely on panoramic X-ray analysis are ineffective. So,a model was developed [21] to recognize the mandibular condyle by categorizing panoramic dental X-ray scans using image recognition methods. First, the panoramic images were gathered retrospectively and 2 different models were applied: (i) the first model called using FRCNN was used to recognize the TMJ-OA and nearby anatomical patterns (such as joint fossa and condyle) and (ii) the other model, namely CNN was used to estimate whether the recognized anatomical area contains any irregularity depending on the shape of the TMJ. Moreover, fine-tuning CNN models such as VGG16, ResNet and Inception were performed to predict the existence or nonexistence of TMJ-OA. But, the major limitation of this model was that the image database was very limited, which influences the recognition efficiency.

Therefore, this article proposes an OGAN model, which creates the synthetic panoramic images related to the TMJ-OA. In this GAN model, the generator is used to produce synthetic panoramic dental images with the optimal hyperparameters, whereas the discriminator is trained to decide whether the created images are realistic-like images or not. The optimal hyperparameters such as training rate, dropout retain probability, batch range and the number of neurons in dense units are selected by using the EHO scheme. The EHO is performed depending on the herding

activities of elephant groups, which is modeled into a clan operator and separating operator for choosing the optimal hyperparameters. Once the OGAN execution is completed, the created synthetic panoramic images are included in the actual database to augment the number of learning and test images. Moreover, the learning images are fed to the FRCNN to capture the condylar area from those images and recognize the abnormalities. Further, the test images are used to validate the trained FRCNN model for TMJ-OA recognition. Thus, training and recognition efficiency is effectively increased by developing the OGAN-FRCNN model using a huge amount of panoramic dental images.

The residual portions of this manuscript are arranged as: section 2 reviews the previous research associated with the TMJ-OA recognition. Section 3 explains the OGAN as image augmentation for TMJ-OA recognition using FRCNN and section 4 displays its efficacy. Section 5 summarizes the whole study and suggests further development.

2. Literature survey

A minimally invasive scheme was designed [22] to diagnose the TMJ-OA disorder. The intention was to analyze the relationship among a collection of biomarkers, which were related to the condylar morphology and to use artificial intelligence for TMJ-OA detection. In this scheme, serum and salivary levels of inflammatory biomarkers were quantified by the protein microarrays. As well, the neural network was trained with other condyles to recognize and categorize the level of TMJ-OA. But, it needs objective quantitative radiomic features of subchondral bone patterns while a large-scale dataset was utilized.

A hybrid graph-cut (HGC) method was developed [23] with CNN to identify dental disorders from radiographic 2D dental images. First, a histogram using an adaptive scheme was utilized in the preprocessing to enlarge the disparity and balance the intensity of the entire X-ray 2D dental images. It was applied to differentiate the forefront teeth and the areas of background bones. Then, those images were split into areas related to the objects. Besides, the HGC partition was applied to partition the oral cavity and its tissues. Those were further learned by CNN to classify dental disorders. But, the number of training and testing images was insufficient to achieve maximum performance.

The efficiency of AlexNet, VGG16 and DetectNet structures for TMJ-OA detection was discussed and analyzed [24] to categorize maxillary impacted supernumerary teeth (IST) in patients with

completely erupted incisors. But, it did not consider patients with mixed dentition, in which the ISTs recognition was complex due to the existence of unerupted permanent teeth. Also, the number of training and testing images was very limited.

A dental defect identification framework was developed [25] by integrating the adaptive CNN (ACNN) and bag-of-visual words (BoVW). At first, the dental X-ray images were preprocessed by transforming them to grayscale before partition, boundary discovery and mask region-of-interest (ROI). Then, oriented FAST and rotated BRIEF with BoVW, speed up robust features (SURF) with BoVW, scale-invariant feature transform (SIFT) with BoVW and VGG16 were performed to capture and preserve the features mined from the images. Such features were further categorized by the logistic regression (LR), support vector machine (SVM), artificial neural network (ANN), decision tree (DT), gradient boosting and random forest (RF). However, this framework was not applicable for a broad variety of multiple and complex dental image databases.

An advanced system was designed [26] to recognize certain points and lines in dental panoramic radiographs. This system has multiple phases: (a) recognizing synthetic patterns by the fuzzy K-means classification, (b) altering a tangent streak to the bottom edge of the bottom jawbone using the surface investigation, grey-level dilation, binarization and tagging, (c) recognizing the mental foramen area and its center using multi-thresholding, binarization, morphological functions and tagging, (d) producing a vertical streak to the tangent across the center of the cerebral foramen area and 2 similar streaks to the tangent via edges on the cerebral foramen crossed by the vertical, (e) moving a scan along the tangent to recognize fused binary points and (f) recognizing the bottom mandible alveolar crest line by identifying the inter-teeth gap based on the saliency and interest points feature interpretation. But, the collected images were very small and needed more characteristics since the detection of mandible crest line was difficult.

A computer vision scheme was designed [27] using artificial intelligence to recognize and categorize different dental restorations in panoramic radiographs. At first, panoramic images were collected and cropped to find the ROI with maxillary and mandibular alveolar ridges. Then, the local adaptive threshold was applied to split the reconstructions and statistical features were obtained according to the shape and grayscale distribution. Further, a cubic SVM with error-correcting output code (ECOC) was applied to classify the features into the different restoration types. But, the number of

training images was limited and the restorations, which were incorrectly detected, did not undergo the classification phase.

A system to categorize jaw tumors were suggested [28] from the X-ray panoramic scans. Initially, the X-ray panoramic scans were acquired and augmented by horizontal flipping and rotation. Afterward, those scans were provided to the pre-trained VGG16 and VGG19 to separate oral and maxillofacial disorders. But, the accuracy was not effective because of very limited training and testing images.

Several supervised machine learning algorithms were suggested [29] for TMJ disorder classification using surface electromyography (SEMG). First, the SEMG scans were gathered and multiple characteristics were mined. Then, the most relevant characteristics were chosen and passed to the AdaBoost, DT, gradient boosting, xtreme gradient boosting and cat boost classification algorithms to recognize the TMJ disorder. But, these algorithms were not suitable for a massive number of dental images.

A range of deep learning structures like DenseNet121, VGG16, InceptionV3 and ResNet50 was recommended [30] to categorize the kind of canine impaction from panoramic dental radiographic images. But, the major drawback of this study was the limited dimension of the annotated database. The collected radiographic images were affected by low resolution and quality, which needs more data preprocessing.

A computer-assisted recognition model was designed [31] using deep CNN to identify the third molar impacted teeth. First, many panoramic scans were collected and randomly partitioned. Then, a single-stage detector such as YOLOv3 was used and a 2-stage detector, namely FRCNN was used, which uses various backbones to finalize the recognition task. But, the major drawback of this model was that the number of scans was inadequate.

2.1 Problem definition

From the literature survey, the problems in the TMJ-OA recognition models are:

- Some models need objective quantitative radiomic characteristics of subchondral bone patterns while utilizing a large-scale dataset.
- Deep learning models can perform well on a large number of training images, i.e., these models require a broad variety of multiple and complex dental image databases.
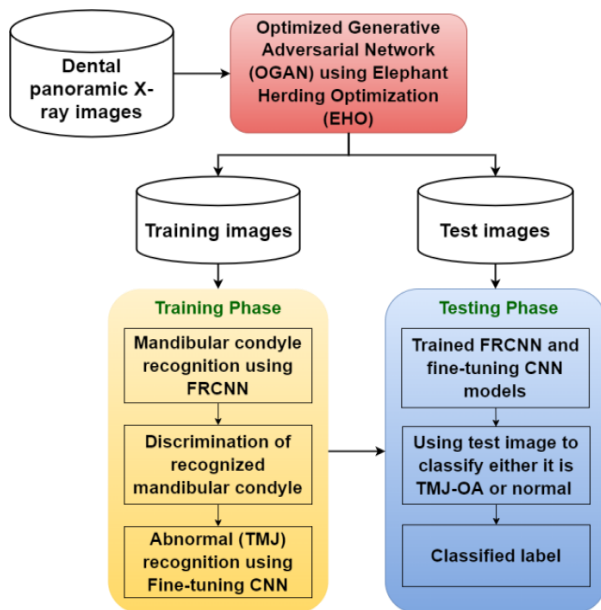
Figure. 1 Flow diagram of the proposed TMJ-OA recognition system

2.2 Research objective

This research focuses on increasing the classification accuracy of TMJ-OA by learning more dental panoramic X-ray images using an optimized adversarial network and deep learning models. The below sections briefly describe the optimization of the adversarial network for image augmentation and TMJ-OA recognition.

2.3 Scientific contribution

According to the literature, most of the existing models are ineffective in terms of limited number of training and testing images. So, this proposed model can alleviate such problem by following major contributions:

1. First, a panoramic dental X-ray image database is obtained and augmented by the OGAN.
2. Then, the augmented images are partitioned into learning and test collections to train and validate the FRCNN with fine-tuning CNN models during the mandibular condylar detection and TMJ-OA recognition stage.

3. Proposed methodology

In this section, the OGAN model as panoramic image augmentation for TMJ-OA recognition is described briefly. Fig. 1 depicts the overall flow of the presented OGAN-FRCNN-based TMJ-OA recognition system.

3.1 Generative adversarial network

Primarily, the GAN is employed for augmenting the number of panoramic dental X-ray images and enhancing the training efficiency. It is engaged in producing artificial images to expand the real image database whilst training FRCNN and fine-tuning CNN models. GANs have been made by the adversarial models to extend the photos in an adversarial way. The configuration of GAN involves a generator G and a discriminator D: (i) G transforms a sample from a random uniform distribution into the picture distribution and (ii) D verifies whether a sample belongs to the actual image distribution. In GANs, G and D are learned independently using the player theory. The weights of G remain constant whereas it creates samples for D to train on and vice versa if it is time to train G.

The discriminator D training task is comparable to that of any other neural network, which classifies both actual and counterfeit samples from G. The discriminator loss function penalizes D to misclassifying an actual sample as counterfeit or a counterfeit sample as actual and modifies D's weights through back-propagation. Likewise, G creates samples, which are categorized by D as being actual or counterfeit. After that, such outcomes are passed to the error factor that punishes G for weakening to deceive D and the back-propagation is utilized to alter G's weights. Fig. 2 illustrates the simple GAN structure.

Because G enhances the training, D's efficiency deteriorates since D unable to discriminate between actual and counterfeit images. When G performs effectively, D achieves an accuracy of 50%. It causes an essential issue for GAN's convergence. When G continues to train after D has given fully random feedback, G learns debris response and its efficiency will be impacted. Normally, G is often a deconvolutional neural network, while D is the CNN if G is extremely accurate, i.e. its error value terminates at 0 and vice versa. Fig. 3 portrays G (deconvolutional neural network) and D (CNN).

Implementation of Basic GAN
Fundamental G in GAN model is illustrated in Fig. 4 (a), whereas every layer in G is portrayed in Fig. 4 (b). Similarly, fundamental D in GAN model is depicted in Fig. 5.

In this model, an Adam optimizer is used, which is a procedure for primary-order gradient-based optimization of stochastic fitness factors, depending on the dynamic measures of low-order moments. It performs well if the cost (loss) function in training is reduced. The loss function for D and G is called
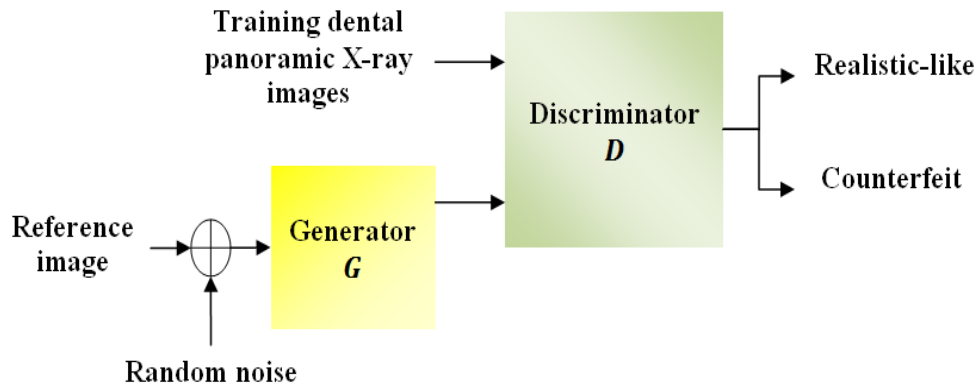
Figure. 2 Panoramic dental image augmentation based on GAN structure
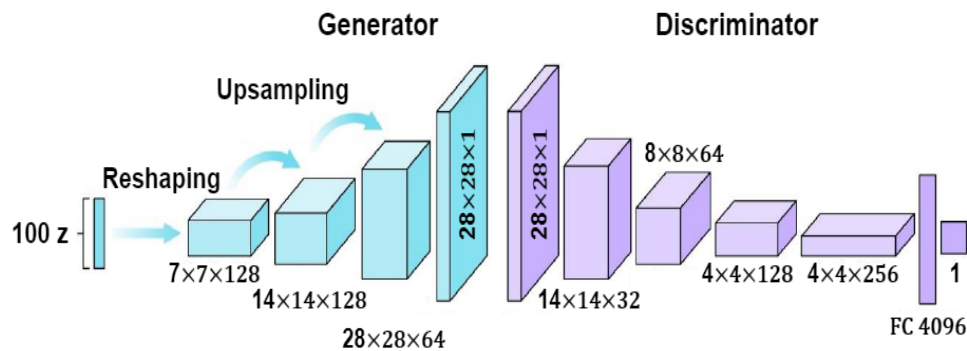

Figure. 3 Generator vs. discriminator

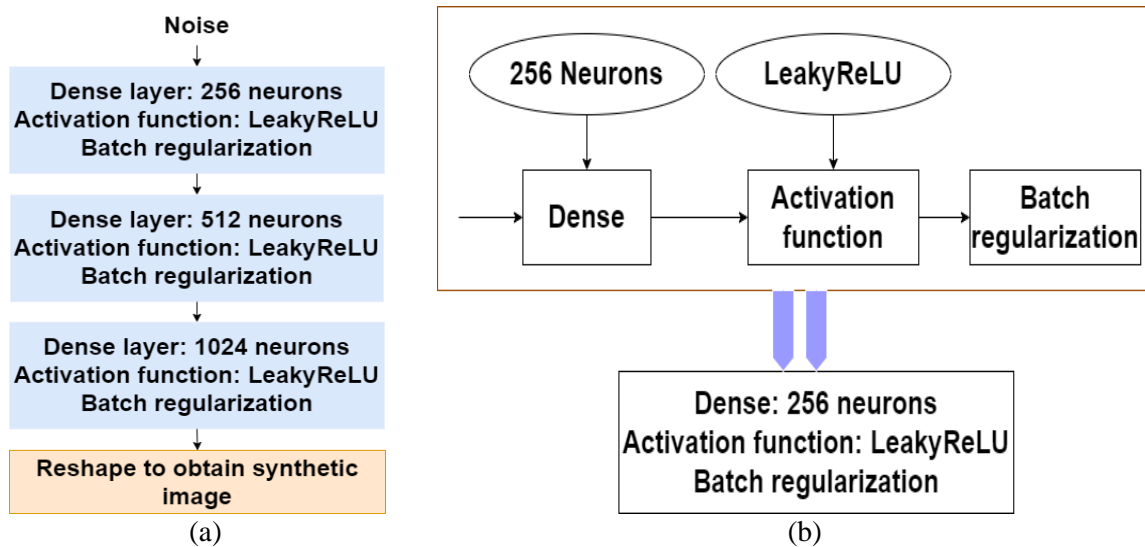(a)   (b)

Figure. 4: (a) design of generator and (b) generator details

binary cross-entropy, which is independent for all classes (vector component), defining that the error determined for all *D* outcome vector elements is unaffected by the ranges of other elements.

So, the knowledge of an image fitted to a specified group must not affect the result for the other group. Since it creates a binary categorization issue among 2 classes in the given database, it is termed binary cross entropy error.

Layer description

The LeakyReLU activation factor is defined by

$$f(i) = \begin{cases} i, & i \geq 0 \\ \alpha \times i, & i < 0 \end{cases} \qquad (1)$$

In Eq. (1), α is set to be 0.2. For batch regularization, momentum defines the significance provided to the shifting mean or the delay in training average and discrepancy, therefore that interference owing to
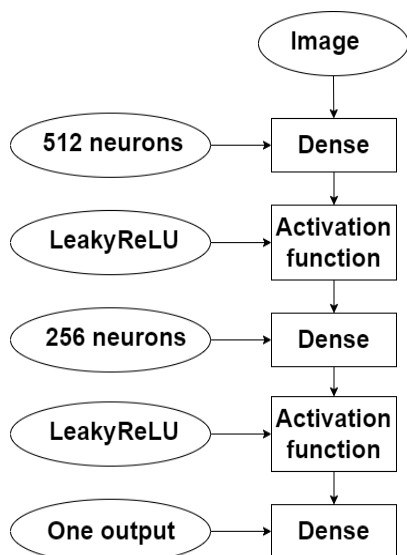
Figure. 5 Design of discriminator

mini-batch is neglected by

$$\mu_{new} = \beta \times \mu_{old} + (1 - \beta)\mu_{current} \quad (2)$$

$$\sigma_{new}^2 = \beta \times \sigma_{old}^2 + (1 - \beta)\sigma_{current}^2 \quad (3)$$

$$\beta = momentum \quad (4)$$

Typically, momentum is assigned a maximum range of roughly 0.99, defining maximum delay and time-consuming. If batch ranges are diminutive, the number of iterations operating can be high. Therefore, maximum momentum may lead to time-consuming, yet robust training of the moving average. On the other hand, if the batch size is larger, the number of iterations is less. As well, the data of mini-batch are generally equal to that of the populace. In this case, the momentum is low, thus the average and discrepancy are modified rapidly. So, a basic principle is that:

- Minimum batch range = Maximum momentum (0.9 - 0.99)
- Maximum batch range = Minimum momentum (0.6 – 0.85)

Additionally, a dropout layer is integrated in D, which neglects neurons during the learning stage of a specific group of neurons based on the keep probability. This keep probability is selected randomly.

3.2 Hyperparameter tuning based on EHO

To achieve effective training of both G and D, the EHO algorithm is introduced to select the GAN's hyperparameters: (1) optimal learning rate, (2) optimal dropout retain probability, (3) optimal batch range and (4) optimum amount of neurons in dense units.

So, the hyperparameter tuning procedure with EHO needs a term to be minimized during EHO implementation. According to the GAN, this model contains G error (G_{loss}), D error (D_{loss}) and D accuracy (D_{acc}): So,

$$min\, G_{loss} \rightarrow min\, D_{acc} \leftrightarrow max\, D_{loss} \quad (5)$$

$$max\, G_{loss} \rightarrow max\, D_{acc} \leftrightarrow min\, D_{loss} \quad (6)$$

By considering these terms, the GAN hyperparameters are optimized by the EHO, which is a new meta-heuristic optimization scheme based on the herding activity of elephants. In the wild, elephants from various clans coexist under the direction of a matriarch and as male elephants mature, they separate from their family units. Such 2 activities are modeled as 2 factors:

3.2.1. Clan factor

In every elephant clan, a matriarch oversees the community's everyday activities. So, for all elephants in a clan C_i, their consecutive location is impacted by matriarch C_i. For the elephant j in C_i, it is fine-tuned by

$$x_{new,C_i,j} = x_{C_i,j} + \alpha \times \left(x_{best,C_i} - x_{C_i,j}\right) \times r \quad (7)$$

In Eq. (7), $x_{new,C_i,j}$ and $x_{C_i,j}$ denote freshly fine-tuned and the previous location for j in C_i, correspondingly, $\alpha \in [0,1]$ indicate the scaling variable, which computes the impact of m_i on $x_{C_i,j}$, x_{best,C_i} is C_i, i.e. the strongest elephant individual in C_i and $r \in [0,1]$. The strongest elephant in all clans is updated by

$$x_{new,C_i,j} = \beta \times \left(x_{center,C_i}\right) \quad (8)$$

In Eq. (8), $\beta \in [0,1]$ indicates the variable, which computes the impact of x_{center,C_i} on $x_{new,C_i,j}$. The expression $x_{new,C_i,j}$ is created by the data obtained by each elephant in C_i.

Additionally, x_{center,C_i} denotes the centroid of C_i and for the dth size, it is determined by

$$x_{center,C_i} = \frac{1}{n_{C_i}} \times \sum_{j=1}^{n_{C_i}} x_{C_i}, j, d \quad (9)$$

In Eq. (9), $1 \leq d \leq D$ indicates the dth size and

Table 1. Lists of notations

Parameters	Ranges
Population size (pop_size)	100
Maximum population (Max_pop)	125
Iteration	1150
$nClan$	5
α	0.25
β	0.05

D denotes its overall size, n_{C_i} denotes the amount of elephants in C_i, x_{C_i}, j, d is the dth of the elephant individual x_{C_i}, j. The center of C_i, x_{center,C_i} is determined through D computations using Eq. (9).

3.2.2. Separating factor

The separating factor at all generations is determined as:

$$x_{worst,C_i} = x_{min} + (x_{max} - x_{min} + 1) \times rand \tag{10}$$

In Eq. (10), x_{worst,C_i} denotes the worst elephant individual in C_i, x_{max} and x_{min} indicate the major and minor boundaries of the elephant individual location, $rand \in [0,1]$ defines the type of stochastic and uniform distribution. The parameter settings for EHO are presented in Table 1.

EHO Algorithm:

Begin

Initialization: Assign $t = 1$, the population size pop_size and the maximum population Max_pop, $\alpha, \beta, nClan$ and the number of elephants for C_i

Evaluate each elephant individual based on its location;

$while(t \leq Max\_pop)$

$for(i = 1\ to\ nClan)$

Rank clan elephants based on their fitness;

$x_{best,C_i} = initial\ elephant;$

$x_{worst,C_i} = last\ elephant$

Execute clan operator;

Execute separating operator;

Examine the inhabitants based on the freshly fine-tuned locations;

Swap the most unpleasant elephant individuals;

$t = t + 1;$

$end\ for$

$end\ while$

Obtain the best solution i.e., best hyperparameters for GAN;

End

Based on the optimal hyperparameters, the GAN is implemented to create the synthetic panoramic dental X-ray images for effective training of the FRCNN and fine-tuned CNN models. Once GAN execution is completed, the created synthetic images are added to the actual database to obtain a new database, which involves a massive amount of panoramic dental X-ray images. Then, this new database is partitioned into learning and test sets. The learning collections are utilized to train the FRCNN and fine-tuning CNN models to recognize the mandibular condyle area and classify TMJ-OA, respectively. Further, the test samples are classified by the trained model into TMJ-OA and normal images.

4. Experimental results

In this section, the effectiveness of the OGAN-FRCNN with fine-tuning CNN is analyzed by implementing it in MATLAB 2019b. In this analysis, a total of 116 panoramic dental X-ray images are taken from https://data.mendeley.com/datasets/hxt48yk462/2. By using OGAN, 6000 images are created in this study. From this database, 65% of images are applied for learning and the residual 35% are applied for testing. Also, a comparative analysis is presented for proposed and existing models: HGC-CNN [23], SVM-ECOC [27], VGG16 [28], VGG19 [28], DenseNet121 [30], InceptionV3 [30], ResNet50 [30], YOLOv3 [31] and FRCNN [21] regarding precision, recall, f-measure and accuracy. The evaluation metrics are described below.

- Accuracy: It is the proportion of exact recognition over the total samples tested.

$$Accuracy = \frac{True\ Positive\ (TP) + True\ Negative\ (TN)}{TP + TN + False\ Positive\ (FP) + False\ Negative\ (FN)} \tag{11}$$

In Eq. (11), the quantity of normal samples properly categorized as normal is TP, while the quantity of TMJ-OA samples properly categorized as TMJ-OA is TN. Also, FP is the quantity of TMJ-OA samples improperly categorized as normal, whereas FN is the quantity of normal samples improperly categorized as TMJ-OA.

- Precision: It determines the correctly recognized labels at TP and FP rates.

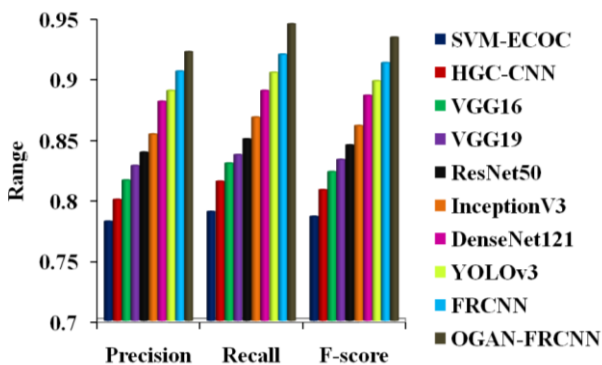$$Precision = \frac{TP}{TP + FP} \tag{12}$$

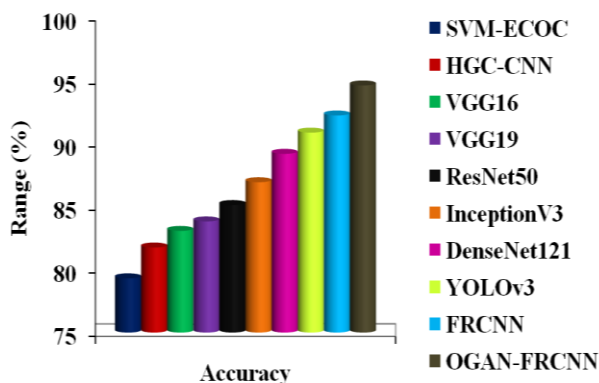Figure. 6 Evaluation of precision, recall & f-measure for proposed and existing TMJ-OA recognition models

Figure. 7 Comparison of accuracy for proposed and existing TMJ-OA recognition models

- Recall: It is the proportion of labels, which are correctly recognized at TP and FN rates.

$$Recall = \frac{TP}{TP+FN} \qquad (13)$$

- F-score (F): It is measured as:

$$F-measure = \frac{2 \times Precision \times Recall}{Precision+Recall} \qquad (14)$$

Fig. 6 illustrates the efficiency of various models applied to the panoramic dental X-ray database to classify the TMJ-OA. It observes that the effectiveness of the OGAN-FRCNN model in terms of precision, recall and f-score is greater than that of other classifier models because of increasing the number of training images. So, this scrutiny indicates that the precision values obtained by the OGAN-FRCNN are 17.9% higher than the SVM-ECOC, 15.3% higher than the HGC-CNN, 13% superior to the VGG16, 11.4% superior to the VGG19, 9.9% superior to the ResNet50, 8% superior to the InceptionV3, 4.7% superior to the DenseNet121, 3.6% superior to the YOLOv3 and 1.8% higher than

the FRCNN.

The recall values obtained by the OGAN-FRCNN are 19.6% larger than the SVM-ECOC, 16% larger than the HGC-CNN, 13.9% larger than the VGG16, 13% larger than the VGG19, 11.2% larger than the ResNet50, 8.9% larger than the InceptionV3, 6.2% larger than the DenseNet121, 4.4% larger than the YOLOv3 and 2.7% larger than the FRCNN. Similarly, the f-score values obtained by the OGAN-FRCNN are 18.8% greater than the SVM-ECOC, 15.6% superior to the HGC-CNN, 13.5% superior to the VGG16, 12.1% superior to the VGG19, 10.5% greater than the ResNet50, 8.5% greater than the InceptionV3, 5.4% greater than the DenseNet121, 4% greater than the YOLOv3 and 2.3% greater than the FRCNN.

Fig. 7 exhibits the accuracy of various models applied to the panoramic dental X-ray database to classify the TMJ-OA. It observes that the accuracy of the OGAN-FRCNN is 19.3% better than the SVM-ECOC, 15.7% better than the HGC-CNN, 13.9% better than the VGG16, 12.9% better than the VGG19, 11.1% better than the ResNet50, 8.8% better than the InceptionV3, 6.1% better than the DenseNet121, 4.2% better than the YOLOv3 and 2.6% better than the FRCNN. Thus, it indicates that the OGAN-FRCNN with fine-tuned CNN models achieves a higher efficacy in detecting mandibular condylar and recognizing TMJ-OA in the X-ray dental images.

Thus, the OGAN-FRCNN can improve the classification of panoramic dental X-ray scans to recognize TMJ-OA patients by augmenting the training and testing sets, whereas all other existing models such as SVM-ECOC, HGC-CNN, VGG16, VGG19, ResNet50, InceptionV3, DenseNet121, YOLOv3 and FRCNN lacks the training and testing image collections.

5. Conclusion

In this paper, the OGAN with a deep learning classification model was designed for panoramic dental X-ray image augmentation and TMJ-OA classification. First, the panoramic X-ray image database was collected and fed to the GAN model to produce the synthetic panoramic X-ray images. In this GAN, the hyperparameters were selected by the EHO algorithm for effective training of both generator and discriminator. Then, those synthetic images are included in the actual database to obtain training and test sets. Later, the FRCNN and fine-tuning CNN models were trained using the training images to detect the condylar area and classify the TMJ-OA. Moreover, the test images were classified by trained model into normal and TMJ-OA. At last,

199

the test outcomes of the OGAN-FRCNN model on panoramic dental X-ray images proved that it has 94.59% accuracy for TMJ-OA recognition in contrast with the existing models.

Conflict of interest

The authors declare no conflict of interest.

Author contributions

Conceptualization, methodology, software, validation, Vijaya Kumar; formal analysis, investigation, Santhi; resources,data curation, writing—original draft preparation, Vijaya Kumar; writing—review and editing, Vijaya Kumar; visualization; supervision, Santhi.

References

[1] H. N. Mohamed, M. S. Ashmawy, M. E. E. Y. Ekladious, and M. M. Farid, "Analysis of the Relationship between Condylar Changes and Anterior Disc Displacement with Reduction: A Preliminary Study", *Oral Radiology*, pp. 1-10, 2020.

[2] I. D. A. F. Muniz, N. L. D. S. Villarim, I. L. A. Ribeiro, A. U. D. Batista, P. R. F. Bonan, and M. A. O. D. Sales, "Is There an Association Between Rheumatoid Arthritis and Bone Changes in the Temporomandibular Joint Diagnosed by Cone-Beam Computed Tomography? A Systematic Review and Meta-Analysis", *Clinical Oral Investigations*, Vol. 25, No. 5, pp. 2449-2459, 2021.

[3] N. Alqhtani, D. Alshammery, N. AlOtaibi, F. AlZamil, A. Allaboon, D. AlTuwaijri, and M. A. Baseer, "Correlations between Mandibular Asymmetries and Temporomandibular Disorders: A Systematic Review", *Journal of International Society of Preventive & Community Dentistry*, Vol. 11, No. 5, pp. 481-489, 2021.

[4] E. A. A. Moraissi, P. C. R. Conti, A. Alyahya, K. Alkebsi, A. Elsharkawy, and N. Christidis, "The Hierarchy of Different Treatments for Myogenous Temporomandibular Disorders: A Systematic Review and Network Meta-Analysis of Randomized Clinical Trials", *Oral and Maxillofacial Surgery*, pp. 1-15, 2021.

[5] F. Oluwajana, P. Clarke, E. F. Thomas, M. James, and C. Crawford, "Temporomandibular Disorders. Part 1: Anatomy, Aetiology, Diagnosis and Classification", *Dental Update*, Vol. 49, No. 4, pp. 320-328, 2022.

[6] G. H. Lee, J. H. Park, S. M. Lee, and D. Moon, "New Definition for Relating Occlusion to Varying Conditions of the Temporomandibular Joint: Conditions of the Temporomandibular Joint Orthodontists Need to Know", *AJO-DO Clinical Companion*, Vol. 1, No. 3, pp. 181-186, 2021.

[7] Q. Auh and Y. H. Lee, "Can the Arthralgia of Temporomandibular Joint Cause Referred Pain?", *Journal of Oral Medicine and Pain*, Vol. 47, No. 1, pp. 72-73, 2022.

[8] G. Dimitroulis, "Surgical Classification for Temporomandibular Joint Disorders", In: *Temporomandibular Joint Disorders*, Springer, pp. 163-169, 2021.

[9] X. Xiong, Z. Ye, H. Tang, Y. Wei, L. Nie, X. Wei, and B. Song, "MRI of Temporomandibular Joint Disorders: Recent Advances and Future Directions", *Journal of Magnetic Resonance Imaging*, Vol. 54, No. 4, pp. 1039-1052, 2021.

[10] R. Arayasantiparb, S. Mitrirattanakul, P. Kunasarapun, H. Chutimataewin, P. Netnoparat, and W. S. Heng, "Association of Radiographic and Clinical Findings in Patients with Temporomandibular Joints Osseous Alteration", *Clinical Oral Investigations*, Vol. 24, No. 1, pp. 221-227, 2020.

[11] A. Whyte, R. Boeddinghaus, A. Bartley, and R. Vijeyaendra, "Imaging of the Temporomandibular Joint", *Clinical Radiology*, Vol. 76, No. 1, pp. 1-15, 2021.

[12] N. Ahmed, M. S. Abbasi, F. Zuberi, W. Qamar, M. S. B. Halim, A. Maqsood, and M. K. Alam, "Artificial Intelligence Techniques: Analysis, Application, and Outcome in Dentistry – A Systematic Review", *BioMed Research International*, Vol. 2021, pp. 1-15, 2021.

[13] T. Kishimoto, T. Goto, T. Matsuda, Y. Iwawaki, and T. Ichikawa, "Application of Artificial Intelligence in the Dental Field: A Literature Review", *Journal of Prosthodontic Research*, Vol. 66, No. 1, pp. 19-28, 2022.

[14] A. M. González, L. R. Calatayud, N. G. D. Oliveira, and J. M. U. Torrent, "Artificial Intelligence in Orthodontics: Where Are We Now? A Scoping Review", *Orthodontics & Craniofacial Research*, Vol. 24, pp. 6-15, 2021.

[15] A. Kumar, H. S. Bhadauria, and A. Singh, "Descriptive Analysis of Dental X-ray Images using Various Practical Methods: A Review", *PeerJ Computer Science*, Vol. 7, pp. 1-41, 2021.

[16] L. Kats, M. Vered, J. Kharouba, and S. Blumer, "Transfer Deep Learning for Dental and Maxillofacial Imaging Modality Classification: A Preliminary Study", *Journal of Clinical*

Pediatric Dentistry, Vol. 45, No. 4, pp. 233-238, 2021.

[17] D. Kim, J. Choi, S. Ahn, and E. Park, "A Smart Home Dental Care System: Integration of Deep Learning, Image Sensors, and Mobile Controller", *Journal of Ambient Intelligence and Humanized Computing*, pp. 1-9, 2021.

[18] J. A. Rodrigues, J. Krois, and F. Schwendicke, "Demystifying Artificial Intelligence and Deep Learning in Dentistry", *Brazilian Oral Research*, Vol. 35, pp. 1-7, 2021.

[19] F. Jubair, O. A. Karadsheh, D. Malamos, S. A. Mahdi, Y. Saad, and Y. Hassona, "A Novel Lightweight Deep Convolutional Neural Network for Early Detection of Oral Cancer", *Oral Diseases*, Vol. 28, No. 4, pp. 1123-1130, 2022.

[20] C. T. Lee, T. Kabir, J. Nelson, S. Sheng, H. W. Meng, T. E. V. Dyke, and S. Shams, "Use of the Deep Learning Approach to Measure Alveolar Bone Level", *Journal of Clinical Periodontology*, Vol. 49, No. 3, pp. 260-269, 2022.

[21] D. Kim, E. Choi, H. G. Jeong, J. Chang, and S. Youm, "Expert System for Mandibular Condyle Detection and Osteoarthritis Classification in Panoramic Imaging using R-CNN and CNN", *Applied Sciences*, Vol. 10, No. 21, pp. 1-10, 2020.

[22] B. Shoukri, J. C. Prieto, A. Ruellas, M. Yatabe, J. Sugai, M. Styner, and L. Cevidanes, "Minimally Invasive Approach for Diagnosing TMJ Osteoarthritis", *Journal of Dental Research*, Vol. 98, No. 10, pp. 1103-1111, 2019.

[23] A. A. A. Kheraif, A. A. Wahba, and H. Fouad, "Detection of Dental Diseases from Radiographic 2D Dental Image Using Hybrid Graph-Cut Technique and Convolutional Neural Network", *Measurement*, Vol. 146, pp. 333-342, 2019.

[24] C. Kuwada, Y. Ariji, M. Fukuda, Y. Kise, H. Fujita, A. Katsumata, and E. Ariji, "Deep Learning Systems for Detecting and Classifying the Presence of Impacted Supernumerary Teeth in the Maxillary Incisor Region on Panoramic Radiographs", *Oral Surgery, Oral Medicine, Oral Pathology and Oral Radiology*, Vol. 130, No. 4, pp. 464-469, 2020.

[25] V. T. N. Ngoc, A. C. Agwu, L. H. Son, T. M. Tuan, C. N. Giap, M. T. G. Thanh, and T. T. Ngan, "The Combination of Adaptive Convolutional Neural Network and Bag of Visual Words in Automatic Diagnosis of Third Molar Complications on Dental X-ray Images", *Diagnostics*, Vol. 10, No. 4, pp. 1-10, 2020.

[26] I. Aliaga, V. Vera, M. Vera, E. García, M. Pedrera, and G. Pajares, "Automatic Computation of Mandibular Indices in Dental Panoramic Radiographs for Early Osteoporosis Detection", *Artificial Intelligence in Medicine*, Vol. 103, pp. 1-38, 2020.

[27] R. A. Aslan, T. Yeshua, D. Kabla, I. Leichter, and C. Nadler, "An Artificial Intelligence System using Machine-Learning for Automatic Detection and Classification of Dental Restorations in Panoramic Radiography", *Oral Surgery, Oral Medicine, Oral Pathology and Oral Radiology*, Vol. 130, No. 5, pp. 593-602, 2020.

[28] A. K. Ismael and A. M. Khidhir, "Evaluation of Transfer Learning with CNN to Classify the Jaw Tumors", In: *IOP Conf. Series: Materials Science and Engineering, IOP Publishing*, Vol. 928, No. 3, pp. 1-7, 2020.

[29] D. S. Bormane and R. B. Kakkeri, "Detection of Temporomandibular Joint Disorder using Surface Electromypgraphy by Supervised Classification Models", *Materials Today: Proceedings*, pp. 1-4, 2021.

[30] M. Aljabri, S. S. Aljameel, N. M. Allah, J. Alhuthayfi, L. Alghamdi, N. Alduhailan, and W. A. Turki, "Canine Impaction Classification from Panoramic Dental Radiographic Images using Deep Learning Models", *Informatics in Medicine Unlocked*, Vol. 30, pp. 1-10, 2022.

[31] M. E. Celik, "Deep Learning based Detection Tool for Impacted Mandibular Third Molar Teeth", *Diagnostics*, Vol. 12, No. 4, pp. 1-13.